Available online at www.sciencedirect.com

SCIENCE DIRECT®

Earth and Planetary Science Letters 231 (2005) 263–277

EPSL

www.elsevier.com/locate/epsl

Multiple mechanisms of remagnetization involving sedimentary greigite (Fe_3S_4)

Andrew P. Roberts*, Richard Weaver[1]

Southampton Oceanography Centre, University of Southampton, European Way, Southampton SO14 3ZH, U.K.

Received 24 June 2004; received in revised form 19 November 2004; accepted 24 November 2004

Editor: V. Courtillot

Abstract

Sedimentary greigite (Fe_3S_4) is being increasingly implicated as the carrier of late diagenetic remagnetizations in fine-grained marine and terrestrial sediments. We have conducted detailed scanning electron microscope observations on polished sections from such sediments, coupled with elemental microanalysis, to identify greigite and to characterize the mode of occurrence and the relationships between the observed greigite and other authigenic and detrital mineral phases. This detailed observational work, in conjunction with recently published work, has enabled identification of several mechanisms for remagnetization involving greigite: (1) neoformation of greigite on the surfaces of early diagenetic framboidal and nodular pyrite; (2) greigite growth within cleavages of detrital sheet silicate grains; (3) neoformation of greigite on the surfaces of authigenic clays (smectite, illite); (4) greigite nucleation on the surfaces of siderite; (5) greigite growth on the surface of gypsum that resulted from earlier oxidation of nodular pyrite. Many other mechanisms for greigite neoformation are conceivable. The key variables are appropriate redox conditions for generation of sulphide and availability of iron from the dissolution of a wide range of possible reactive detrital and authigenic iron-bearing minerals. Documentation of a wide range of mechanisms for neoformation of greigite provides compelling evidence that sediments containing greigite should be routinely suspected of remagnetization, which will complicate or compromise studies of environmental magnetism and geomagnetic field behaviour.

Keywords: greigite; iron sulphide; pyrite; diagenesis; remagnetization; silicate; siderite; gypsum

1. Introduction

The iron sulphide mineral greigite (Fe_3S_4) is a thiospinel [1], which shares the same crystal structure as magnetite (Fe_3O_4) and is therefore strongly ferrimagnetic. Greigite forms authigenically in anoxic sedimentary environments as a precursor to pyrite (FeS_2) in association with chemical reactions

* Corresponding author. Tel.: +44 23 8059 3786; fax: +44 23 8059 3059.

E-mail address: arob@soc.soton.ac.uk (A.P. Roberts).

[1] Now at: Offshore Hydrocarbon Mapping Plc, The Technology Centre, The Offshore Technology Park, Claymore Drive, Bridge of Don, Aberdeen AB23 8GD, U.K.

0012-821X/$ - see front matter © 2004 Elsevier B.V. All rights reserved.
doi:10.1016/j.epsl.2004.11.024

driven by bacterial degradation of organic matter [e.g., [2–6]]. Microbes reduce sulphate to provide energy to oxidize organic matter. This process releases sulphide (H_2S or HS^-), which reacts with detrital iron-bearing minerals [e.g., [7,8]] to form pyrite. Pyrite is ubiquitous in anoxic marine sediments [e.g., [2]] in which there is an abundant supply of sulphate and where iron is readily available in sedimentary pore waters through dissolution of reactive detrital iron-bearing minerals. Pyrite is also abundant in terrestrial sediments deposited under anoxic conditions [2].

As a common precursor to pyrite [2–6], greigite will have originally been present in a large proportion of the world's sedimentary rocks; this has important implications for the magnetization of these rocks. In the presence of abundant pore water sulphate, which is typical of most marine environments, pyritization reactions would be expected to go to completion and greigite would not be expected to persist in the geological record. Nevertheless, extremely small amounts of magnetic material can be paleomagnetically important (parts per billion concentrations can be detected with modern magnetometers). Most geochemical studies are not able to detect such potentially small concentrations of phases like greigite, and it is therefore often ignored in sedimentary studies of pyritization. In contrast, the sensitivity of magnetic analysis has led, over the last 15 years, to a major increase in recognition of the importance and persistence of greigite in the geological record. In some cases, greigite is observed to be the only magnetic mineral present in marine sediments that were deposited under anoxic conditions. In extreme cases, greigite is the only magnetic mineral observed over substantial stratigraphic thicknesses (hundreds of metres) over large areas (hundreds of km^2) [e.g., [9,10]]. Geochemical analysis of these sediments indicates that greigite preservation is favoured by high concentrations of reactive iron and by low concentrations of organic carbon. In such cases, high iron activity can remove the H_2S produced by microbial degradation of organic matter so effectively that pyritization is retarded or arrested and greigite is preserved [11].

Under the conventional view that pyritization reactions occur during early diagenesis at shallow burial depths [e.g., [2]], it would be reasonable to expect any greigite that persists in the geological record to carry a more or less syn-depositional magnetization [e.g., [12,13]]. In contrast to this view, numerous studies have shown that greigite can be responsible for late diagenetic remagnetizations that compromise paleomagnetic and environmental magnetic studies [e.g., [10,14–18]]. Even in a best-case scenario of an active depositional environment where one might expect a syn-depositional magnetic signal, Liu et al. [19] showed that greigite can authigenically form at depths of 3–30 m below the sediment/water interface. Together, this evidence suggests that greigite cannot be assumed to provide reliable information about geological or geophysical processes that relate to the time of sediment deposition. In this paper, we provide support for this view by documenting evidence for numerous remagnetization mechanisms involving greigite. Much of the evidence has been published as part of individual case studies, but a systematic synthesis of the known mechanisms for remagnetization involving greigite has not been presented before. We present such a synthesis along with an overview of the forcing events that can give rise to remagnetizations involving greigite.

2. Geochemical classification of sedimentary environments

Before presenting our results, we summarize a standard scheme for geochemical classification of sedimentary environments [20] to provide a framework for interpretation of results. Decomposition of buried organic matter produces an important series of reactions that are characteristic of different diagenetic zones in the sediment column (Fig. 1). As organic matter is oxidized (oxic conditions), the concentration of dissolved oxygen in the sediment is reduced to almost zero (producing suboxic conditions). Once oxygen is consumed, oxidation proceeds by using the next most efficient oxidant until all oxidants are depleted or until the organic carbon supply is consumed [21]. This sequence involves consumption of nitrate and labile manganese oxides, followed by reduction of iron oxide (all under suboxic conditions), and then by sulphate reduction and methano-

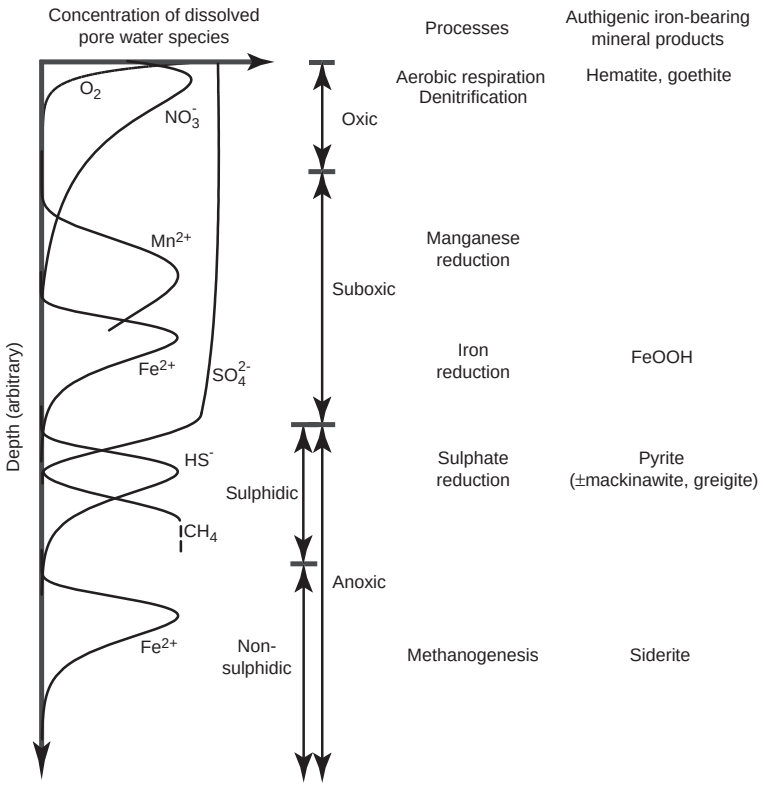

Fig. 1. Geochemical classification scheme for sedimentary environments, with idealized concentration profiles for dissolved pore water species with respect to depth, and the authigenic iron-bearing minerals expected to form in the respective diagenetic zones. Depth is arbitrary; the depth positions of real concentration profiles will depend largely on sedimentation rate and supply of (reactive) organic matter. Profiles are shown for both the reactants (O_2, NO_3^-, SO_4^{2-}) and the products (Mn^{2+}, Fe^{2+}, HS^-, CH_4) in the redox zonation. Modified from Froelich et al. [21], Berner [20], and Kasten et al. [61].

genesis (under anoxic conditions). Iron-bearing minerals are intimately associated with organic matter decomposition, as shown on the right-hand side of Fig. 1. Iron reduction results in an increase in dissolved iron concentrations in sedimentary pore waters and sulphate reduction results in a decrease in sulphate to near-zero values in totally anoxic pore waters and to an increase in dissolved sulphide (H_2S and HS^-). These dissolved species react to form pyrite, including precursor phases such as mackinawite ($Fe_{1+x}S$) and greigite. In anoxic, non-sulphidic environments, dissolved iron will build up in the interstitial waters, but it cannot react to form pyrite if sulphide is no longer being produced. The reduced iron will therefore be available to precipitate with other ions in solution. If the interstitial waters are saturated with respect to carbonate, siderite ($FeCO_3$) can form. Using this geochemical scheme, the presence of different authigenic iron-bearing mineral phases can be used to indicate the diagenetic stages through which the sediment has progressed [20]. As shown below, formation of greigite during late diagenesis requires disruption of this steady-state diagenetic progression through the influence of some external forcing event.

3. Methods

Iron sulphide minerals can be easily identified using a scanning electron microscope (SEM) because of their high electron backscatter and obvious microtextures. Identification of microtextural relationships using an SEM can therefore provide

important evidence concerning remagnetization mechanisms [e.g., [17,18,22]]. In each of the cases to be discussed in the present paper, remagnetizations were inferred on the basis of magnetic measurements; however, SEM observations were needed to document evidence for the remagnetization mechanism and to confirm that the authigenic greigite grew as a result of late diagenetic reactions. The mechanisms documented in this paper involve rapidly deposited siliciclastic marine and terrestrial sediments from Taiwan, Antarctica, and Italy. The depositional age of the sediments ranges from early Miocene to middle Pleistocene.

Sediment microtextures were investigated using resin-impregnated polished sections of bulk sediment samples in order to identify mechanisms for the documented remagnetizations. A LEO 1450VP SEM, operated at 20 keV at the Southampton Oceanography Centre, was used for these observations. All of the polished sections were taken from sediment cores and were oriented perpendicular to the bedding plane to help identify whether authigenic phases have been affected by sediment compaction. Elemental analyses were obtained using an X-ray energy-dispersive spectrometer (EDS). Point analyses of individual mineral grains, or of clusters of grains, were carried out using a Princeton Gamma Tech (IMIX-PTS) system (2–3 μm beam diameter). A pyrite standard was used to calibrate the analyses. EDS spectra have a high ratio of iron to sulphur for greigite (43% (at.%) Fe; 57% S) compared to pyrite (33% Fe; 67% S), which makes it straightforward to clearly identify the two phases (Fig. 2). Greigite would be expected to have a higher electron backscatter than pyrite because of its higher atomic weight. However, much of the observed greigite is very fine-grained and has a darker contrast, probably because it has less regular surfaces that scatter electrons compared to the smoother surfaces of coarser pyrite grains. While the iron to sulphur ratio for monoclinic (magnetic) pyrrhotite (Fe_7S_8) (47% Fe; 53% S) is close to that of greigite, these minerals can be distinguished from each other on the basis of calibrated EDS results (see [17,18,22]). In addition, these phases usually have distinct morphologies (pyrrhotite is typically platy, while greigite occurs as cubo-octahedra), which aid discrimination. All of these factors make SEM observation, coupled with EDS analysis, a powerful tool for investigating remagnetizations involving iron sulphides.

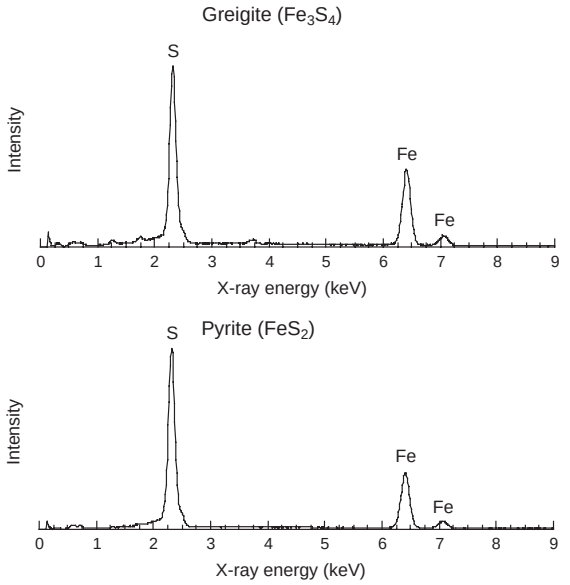

Fig. 2. Representative X-ray energy dispersive spectra for greigite and pyrite, respectively, obtained from samples from the base of the CRP-1 drill-hole, Antarctica (see Sagnotti et al. [18] and the back-scattered electron images shown in Figs. 4 and 5).

4. Remagnetization mechanisms involving sedimentary greigite

Below, we provide evidence for 5 remagnetization mechanisms involving sedimentary greigite. The first 3 mechanisms were documented by Jiang et al. [17] who carried out the first detailed microtextural investigation of remagnetizations carried by greigite. Jiang et al. [17] focused on microtextural observations and on the different modes of greigite occurrence. Here, we emphasize the different remagnetization mechanisms suggested by the observations of Jiang et al. [17] and we describe 2 additional mechanisms that we have documented as part of other studies aimed at understanding the geochronology of the sediments in question. A more detailed description of these 2 mechanisms is given below to provide a coherent synthesis of the known mechanisms for remagnetization involving greigite.

It is important to note that greigite has been inferred to form as a precursor to pyrite through a

variety of geochemical pathways [e.g., [3–6]]. Our results are observational and do not provide evidence concerning the specific pathway by which the greigite formed (e.g., the H_2S pathway, the "polysulphide" pathway, the ferrous iron loss pathway, or the monosulphide oxidation pathway [6]). Regardless of the formation pathway, Kao et al. [11] showed that high iron activity can remove any H_2S produced by microbial activity so effectively that pyritization is retarded or arrested thereby allowing the persistence of greigite in the geological record. We assume that similar processes acted in the sediments where we have observed remagnetizations involving greigite. To avoid confusion with possible pathways for greigite formation, which we do not seek to address, we consistently refer to remagnetization mechanisms in this paper. We use the term mechanism to refer to the mineralogical transformations that took place to provide the necessary dissolved iron and sulphide that became available to form the greigite that remagnetized the host sediment, regardless of the geochemical pathway involved.

4.1. Mechanism 1: neoformation of greigite on pyrite surfaces

Jiang et al. [17] showed that neoformation of greigite occurred on pyrite surfaces in early Pliocene marine sediments from Taiwan. They observed that greigite occurs within iron-sulphide-dominated concretionary nodules that are surrounded by silicate-dominated matrix grains. The detrital silicate grains are embayed by authigenic pyrite overgrowths, which are then enclosed by greigite aggregates. Both the embayed silicate and pyrite grains have partially dissolved edges, which indicates that these grains provided reactants for the subsequent authigenic overgrowth. The observed replacive growth textures strongly suggest that the greigite formed via neoformation on pyrite surfaces. Pyrite is a stable phase under anoxic conditions, so Jiang et al. [17] suggested that the observed partial pyrite dissolution occurred via reaction with oxidants, such as oxidizing acids, Fe^{3+}, or molecular halogens [23]. The release of iron and sulphur from this process is likely to have provided the reactants for the neoformation of greigite. We have observed greigite that has grown on the edges of pyrite framboids within polyframboidal aggregates in most of the sediments that we have analysed (e.g., Fig. 3a). Our observations are consistent with the possibility that this is a widespread mechanism for remagnetization involving greigite.

4.2. Mechanism 2: neoformation of greigite within cleavages of detrital sheet silicate grains

Canfield et al. [8] calculated the reactivity of various iron-bearing detrital mineral phases toward sulphide. The most common sheet silicates (biotite, chlorite, smectite, illite) react more slowly than the most reactive iron oxyhydroxides by about a factor of

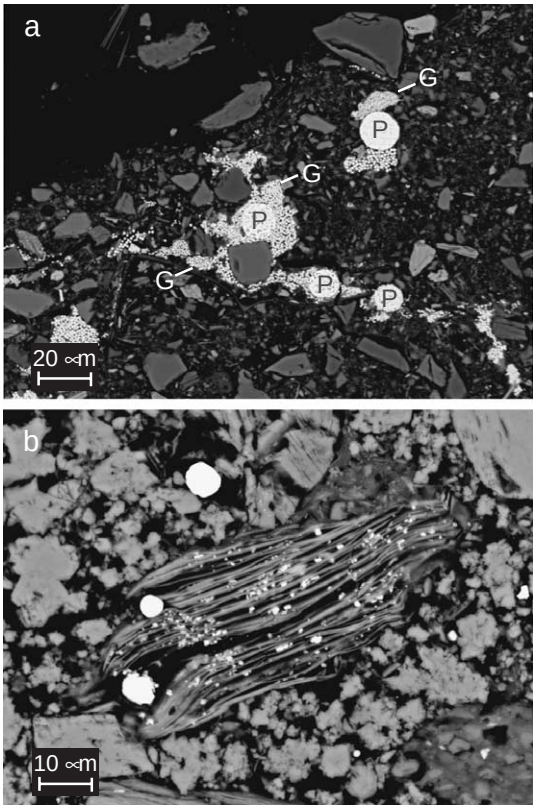

Fig. 3. Representative back-scattered electron image of: (a) greigite neoformation on the outer edges of pyrite from the remagnetized lower part of the CRP-1 core (the sample is from 145.69 mbsf; see Roberts et al. [27] and Sagnotti et al. [18]), and (b) neoformed greigite within cleavages of detrital sheet silicate grains. The sample is a lower Pleistocene terrestrial mudstone from a depth of 43.20 m in core VVM from the paleo-Tiber Valley (see Florindo et al. [45]). Examples of greigite neoformation on the surface of pyrite can also be seen in Fig. 6a and c.

10^8 and they react more slowly than magnetite by about a factor of 10^3. The half-life of reaction of sheet silicates with sulphide is 120,000 yr when in contact with 1 mM concentrations of sulphide (i.e., equivalent to the dissolved sulphide concentrations when most pore water sulphate has been consumed). In such cases, iron sulphide formation is limited by the availability of reactive iron. Even though dissolution of silicates is generally slow, reaction of iron in sheet silicates can result in pyrite formation, as observed under the SEM by Canfield et al. [8]. The large surface area of layers within sheet silicates provides abundant reactive sites for greigite formation over the long time spans envisaged with this mechanism. If greigite is preserved within the layers of sheet silicates as a result of slow reaction of iron with dissolved sulphide, this will have major implications for the paleomagnetic record of such sediments [17].

We have observed greigite and/or pyrite that has grown within silicate sheets in most of the remagnetized greigite-bearing sediments that we have subjected to SEM investigations (e.g., Fig. 3b). Furthermore, X-ray diffraction analyses of greigite-bearing sediments indicate that greigite commonly coexists with chlorite [e.g., [12–14,24]]. It is therefore conceivable that the intimate co-occurrence of these phases resulted from greigite growth within chlorite sheets. The slow kinetics of sheet silicate dissolution strongly supports the interpretation that greigite associated with detrital sheet silicates must have grown late enough not to have produced a syn-depositional magnetization. This mode of greigite growth therefore has the potential to be a widespread remagnetization mechanism.

4.3. Mechanism 3: neoformation of greigite on surfaces of authigenic clays

The third remagnetization mechanism documented by Jiang et al. [17] involves neoformation of greigite on the surfaces of authigenic clays. This mechanism is similar to mechanism 2 in that both involve greigite growth on the surfaces of sheet silicate grains. However, in this case, greigite has grown on the surface of authigenic grains rather than on detrital grains. This directly indicates a late stage remagnetization compared to the case of detrital sheet silicates, where the inference is based on the slow kinetics of dissolution of the iron-bearing silicates. From their observations of early Pliocene marine sediments from Taiwan, Jiang et al. [17] observed intergrowths of greigite with fine-grained iron-rich clays that occur in the peripheral regions of iron sulphide nodules. The iron-rich clays probably consist of a mixture of chlorite and minor illite/smectite and they occur only in the vicinity of greigite, where they fill space between the greigite and corroded silicate grains. These observations are consistent with an origin via diagenetic neoformation. As was pointed out above for mechanism 2, the observation that greigite commonly coexists with chlorite [e.g., [12–14,24]] could conceivably result from greigite growth within the sheets of authigenic clays as well as within detrital silicates.

4.4. Mechanism 4: greigite growth on surfaces of siderite

SEM observations of remagnetized early Miocene glacimarine sediments from the CRP-1 core from McMurdo Sound, Ross Sea, Antarctica, provide microtextural evidence for a progression of diagenetic conditions that caused the successive authigenic growth of pyrite, followed by siderite, and then greigite [18]. Evidence for this sequence of authigenic mineral growth, which resulted in a remagnetization carried by greigite, is provided in Fig. 4. Patches of siderite cement, as shown in low (Fig. 4a) and high (Fig. 4b) magnification views, are evident in all remagnetized samples (light grey). This siderite cement is not the earliest authigenic mineral to have formed because it has clearly overgrown early diagenetic pyrite framboids (circular in cross-section, with bright electron backscatter; Fig. 4c,d). Higher magnification views provide evidence that greigite octahedra grew on the surfaces of the siderite cement (Fig. 4e,f). These observations demonstrate that the greigite did not form during early diagenesis, and that its later diagenetic formation is responsible for the documented remagnetization.

A variation to this scenario is observed in the remagnetized portion of the CRP-1 core. In some cases, pyrite nodules are observed (Fig. 5a). The pyrite in the nodules is euhedral rather than framboidal (Fig. 5a–d). Raiswell [25] suggested that framboidal and euhedral pyrite form in a paragenetic

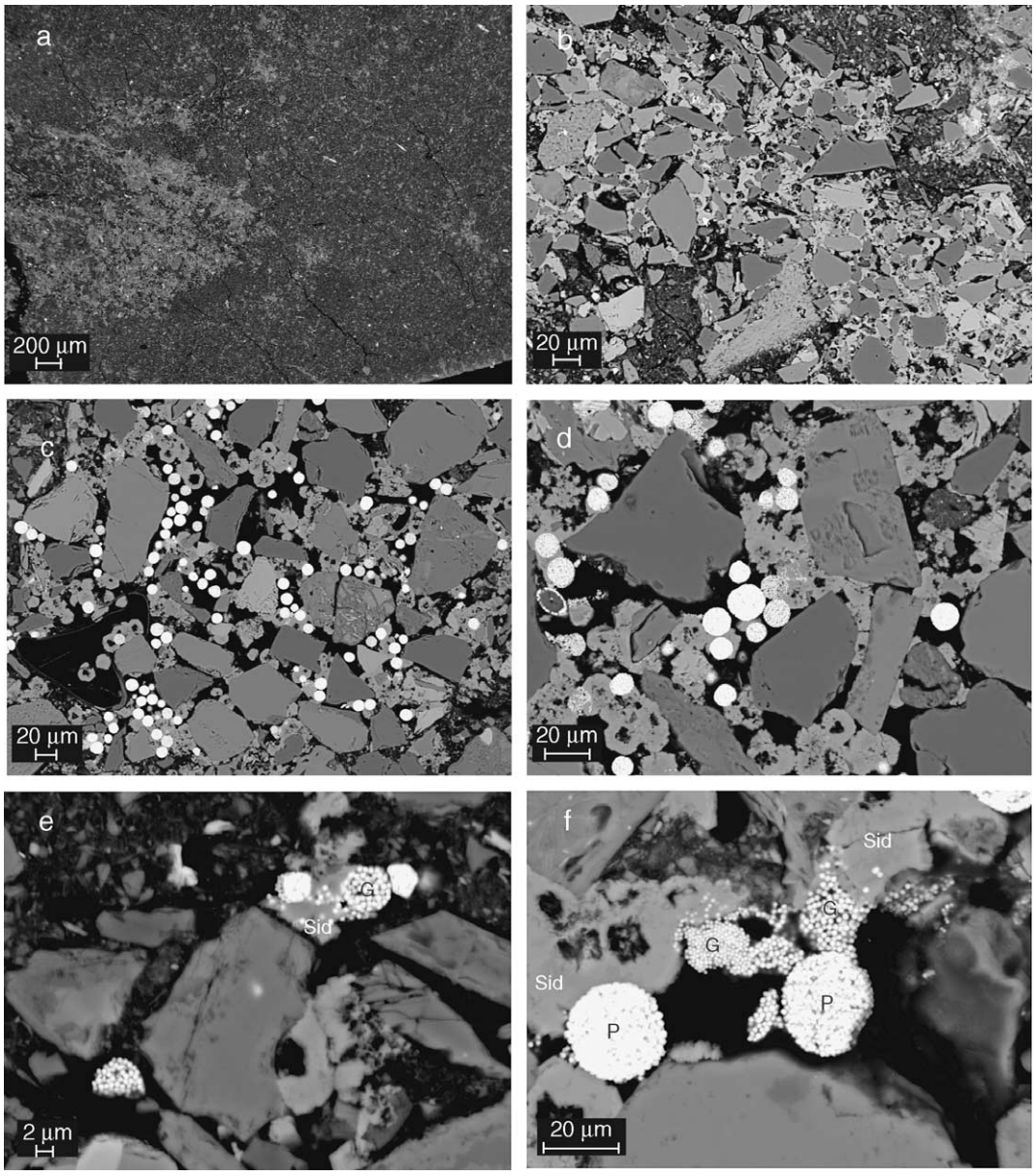

Fig. 4. Representative back-scattered electron images of remagnetized samples (greigite formation from siderite) from the lower part of the CRP-1 core (see Roberts et al. [27] and Sagnotti et al. [18]). (a) Low magnification view of patchy (light grey) siderite cement for a sample from 144.67 m below sea floor (mbsf). (b) Higher magnification view illustrating how siderite has filled and cemented the interstices between detrital grains for the same sample. (c,d) Illustration of the overgrowth of early diagenetic pyrite framboids (bright, with circular cross-section) by the later siderite cement for a sample from 146.63 mbsf. (e,f) Close-up views of the interrelationship of siderite, pyrite, and greigite for samples from 144.67 and 146.63 mbsf, respectively; Sid—siderite, P—pyrite, G—greigite. The siderite has grown between detrital grains, and around pyrite framboids, but the greigite consistently appears on the surface of the siderite cement.

sequence as a result of evolving pore water chemistry. Framboidal pyrite would be expected to grow early in the presence of abundant reactive iron. As reactive iron gets exhausted and sulphate reduction rates become slow, euhedral pyrite is more likely to directly form without a greigite precursor

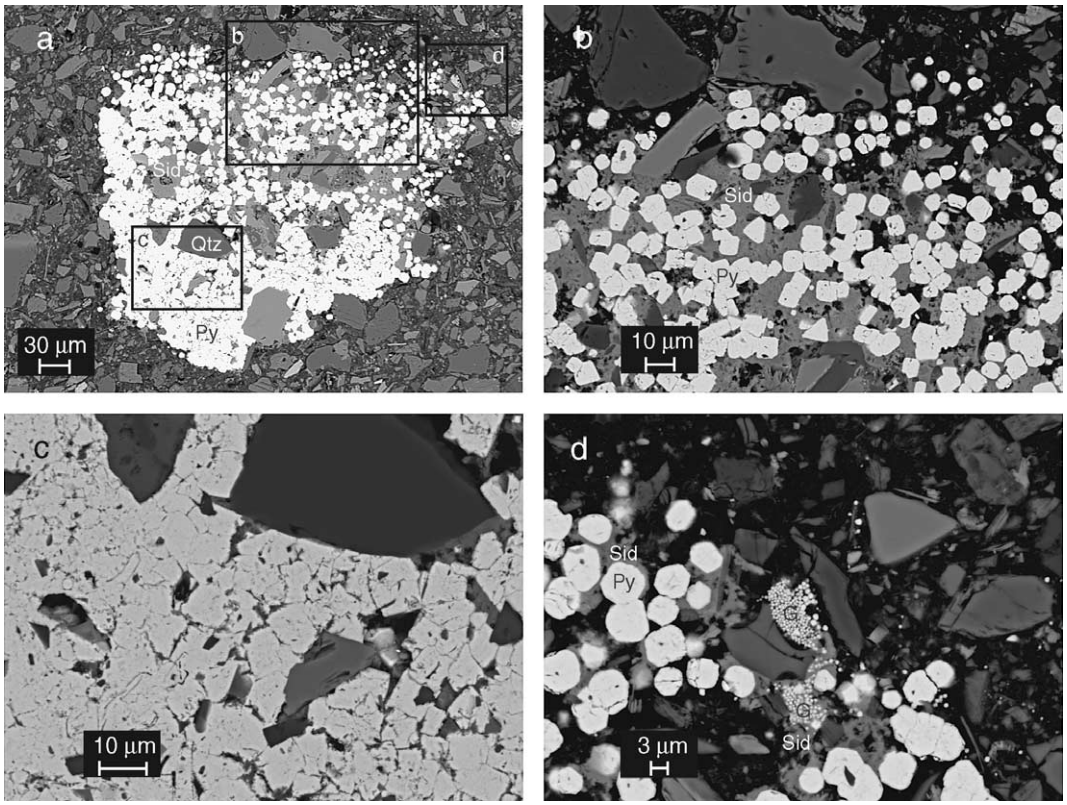

Fig. 5. Representative back-scattered electron images of a remagnetized sample (greigite formation from siderite) from 147.64 mbsf in the lower part of the CRP-1 core. (a) Low magnification view of a pyrite nodule, where euhedral pyrite has grown around detrital grains. The positions of images (b), (c), and (d) are marked by boxes. (b) Higher magnification view illustrating the overgrowth of euhedral pyrite grains by siderite. (c) View of the lower part of the nodule illustrating the dense intergrowth of euhedral pyrite grains. (d) View of the upper part of the nodule illustrating the sequence of authigenic mineral growth in these sediments. Greigite has grown on the surfaces of siderite that has overgrown the euhedral pyrite.

as a result of a kinetic influence on pyrite texture [25]. This suggests that the studied sediments have been subjected to either a prolonged early diagenetic sulphidization event resulting from evolving pore water compositions or to more than one sulphidization event. The fact that the siderite cement overgrew (and therefore post-dates) the euhedral pyrite (Fig. 5a,b) suggests the former. Again, greigite has grown on the surface of siderite grains and is apparently the last-formed authigenic mineral phase (Fig. 5d). Siderite distributions in the lower part of the CRP-1 core are patchy (e.g., Fig. 4a), which is a common mode of growth for siderite cements [e.g., [26]]. This observation explains the alternation between detrital and late diagenetic magnetizations that produced the apparent alternation of polarities observed by Roberts et al. [27] for the lower part of the CRP-1 core.

The geochemical classification scheme of Berner [20] for sedimentary environments (Fig. 1) provides a framework for interpretation of the observed sequence of authigenic mineral growth. The framboidal pyrite will have formed during early diagenetic sulphate reduction. The euhedral pyrite probably post-dates the framboidal pyrite and represents an early diagenetic product that precipitated from more evolved pore waters, as suggested by Raiswell [25]. The later growth of siderite is likely to have occurred during methanogenesis when the sediment was buried deeper in the sediment column. Ongoing iron reduction results in build-up of iron in the interstitial waters, which cannot react to form

pyrite if sulphide is no longer being produced. If the interstitial waters are saturated with respect to carbonate, the presence of reduced iron will enable siderite to form. Formation of greigite requires dissolved sulphide, therefore its formation after siderite would require a change in pore water chemistry that disrupted the geochemical classification scheme of Berner [20]. Siderite contains abundant reactive iron, and, if pore waters become sulphidic, it will react with dissolved sulphide to enable formation of iron sulphides. For example, laboratory synthesis of the iron sulphide mineral smythite (Fe_9S_{11}) makes use of the reactivity of iron in siderite to enable precipitation of smythite under sulphidic conditions [28,29]. A reaction for greigite formation from siderite is given by [30]:

$$3FeCO_3 + 4H_2S \Leftrightarrow Fe_3S_4 + 3H_2CO_3 + H_2. \quad (1)$$

Sediments recovered in the CRP-1 core were never deeply buried [31]. The changes in pore water chemistry required to form greigite after siderite could therefore have been induced by changes in the subsurface position of the interface between fresh terrestrial ground water and saline marine pore waters as a result of large amplitude changes in relative sea level. Alternatively, the change in pore water chemistry could have been driven by glaciotectonically forced fluid migration due to over-riding of glaciers during ice advance events in this ice-proximal Antarctic environment. In contrast to the scheme of Berner [20], Raiswell [32] argued that pore waters can contain small amounts of H_2S throughout the progression of diagenetic stages, and that small amounts of pyrite (and therefore greigite) can form throughout diagenesis, even in the methanogenic zone. Interaction of highly reactive iron on the surface of siderite grains and small residual amounts of pore water H_2S could therefore have enabled greigite formation and the associated remagnetization without a major change in pore water chemistry.

Postma and Jakobsen [33] argued that the widely accepted redox zonation of Berner [20] does not always apply and that diagenetic iron reduction and sulphate reduction can occur simultaneously. Pye et al. [34] demonstrated that siderite and greigite can form simultaneously in sediments where the rate of iron reduction exceeds the rate of sulphate reduction, although such a scenario is less likely in an ancient diagenetic setting where the rates of microbial activity are likely to be much lower than in a modern salt marsh environment. We cannot distinguish between these alternative suggested diagenetic conditions for greigite formation because no pore water geochemical data are available for the CRP-1 core. However, a major change in pore water chemistry is likely because the greigite occurs on the surfaces of siderite grains and therefore appears to have grown after siderite. Siderite cements occur in several parts of the CRP-1 core [31,35], but the lowermost interval is the only one in which we have identified authigenic greigite. This observation supports our interpretation that pore water conditions were different in the lower part of the CRP-1 core.

Remagnetization of sediments as a result of late diagenetic growth of greigite from siderite has not been previously documented, although greigite and siderite commonly co-occur in active depositional/diagenetic environments [e.g., [34,36,37]]. There have also been occasional reports of their co-preservation in the geological record [e.g., [30,38,39]]. Co-occurrences of siderite and other magnetic iron sulphides in the geological record, such as smythite or pyrrhotite [[29,40–42] and references therein] also suggest that this remagnetization mechanism could be relatively widespread in some diagenetic environments. Finally, documentation of siderite and two generations of pyrite that formed as a result of late diagenetic fluid migration events in Paleozoic rocks in Spain [43] suggests that the proposed remagnetization mechanism is feasible in carbonate-bearing rocks if greigite grows as a result of migration of sulphidic fluids through the rocks.

5. Mechanism 5: greigite growth on surfaces of gypsum

Alternating depositional cycles of terrestrial gravels and clays from coastal settings in the paleo-Tiber Valley, southwest of Rome, Italy, have been interpreted to have resulted from large amplitude sea level changes [44]. The presence of abundant volcanic ashes in these sediments provides an excellent opportunity for dating major climatic transitions using $^{40}Ar/^{39}Ar$ geochronology and paleomagnetism.

High precision $^{40}Ar/^{39}Ar$ dates suggest that middle Pleistocene terrestrial clays from the paleo-Tiber Valley have been remagnetized [45]. Our SEM observations verify that greigite is responsible for the observed remagnetization.

The sediments contain patches of iron sulphide aggregates and/or nodules with dimensions of 10's to 100's of μm across (Fig. 6a–f). The aggregates usually contain spherical (circular in cross-section) pyrite framboids made up of reasonably large (~1 μm) pyrite octahedra, as well as less regularly shaped aggregates of pyrite and much finer-grained greigite crystals (Fig. 6a–c). These polyframboidal aggregates are relatively common, and probably result from pyritization of organic matter (carcasses or plants), as suggested by Raiswell [25]. These aggregates often provide similar microtextural evidence to that shown in Fig. 3a, where greigite has neoformed on the surfaces of earlier diagenetic framboidal pyrite (remagnetization mechanism 1). In addition to these polyframboidal aggre-

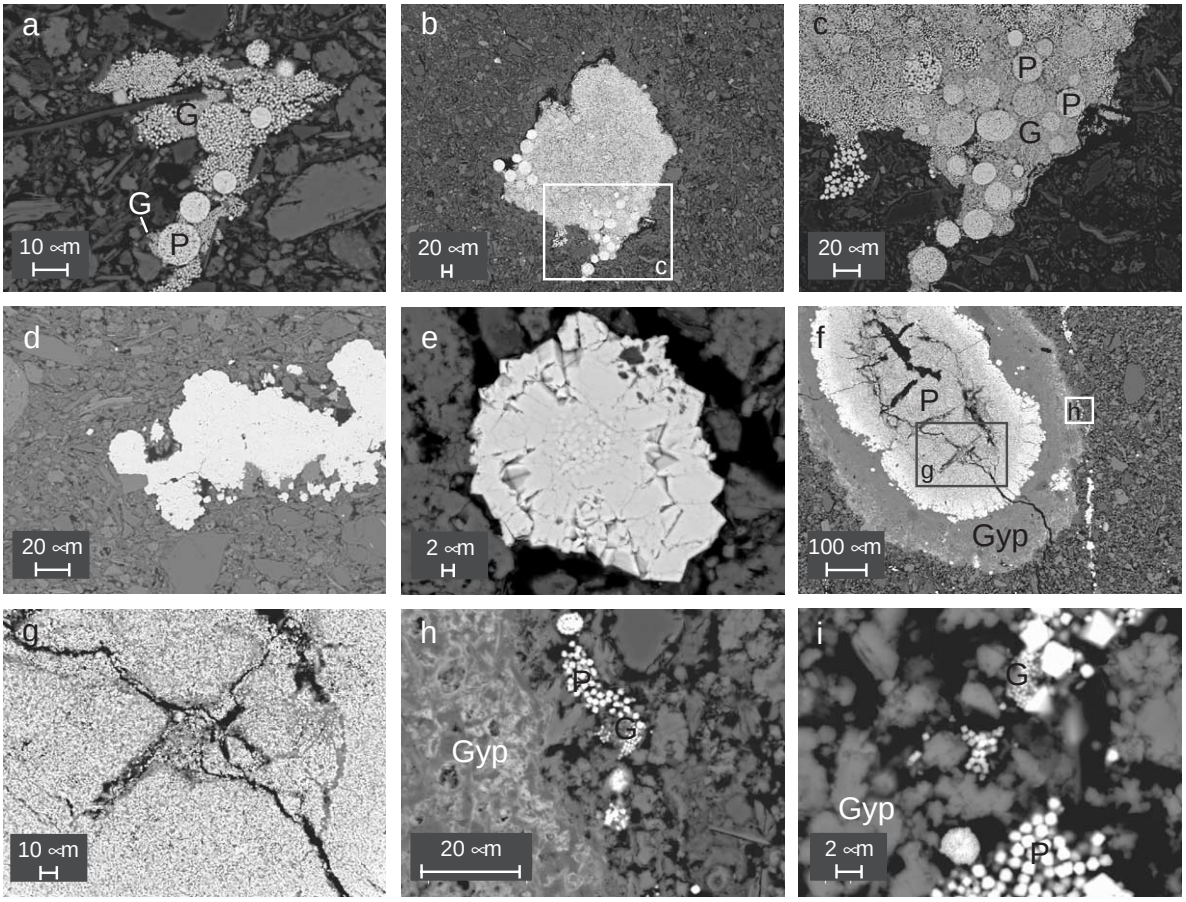

Fig. 6. Representative back-scattered electron images of greigite that formed from gypsum after oxidation of pyrite. The samples are from middle Pleistocene terrestrial clays from the paleo-Tiber Valley, near Rome (see Florindo et al. [45]). (a–c) Polyframboidal aggregates containing both pyrite (coarser grained) and greigite (finer grained) (samples are from 35.7 and 54.24 m in cores PSA and VVM, respectively; the location of image (c) is shown by the box in image (b)). (d,e) Overgrowth of framboidal pyrite by later euhedral pyrite (samples are from depths of 35.7 and 39.2 m in core PSA). Individual framboidal pyrite grains are evident in the middle of image (e). (f) Pyrite (P) nodule with oxidized surface on which gypsum (Gyp) has formed, with greigite and pyrite crystals evident (high electron back-scatter) on the edges, and within, the gypsum. The positions of images (g) and (h) are shown by boxes, all of which are from a sample from a depth of 43.20 m in core VVM. (g) Microcrystalline mass of pyrite in the core of the nodule. (h,i) Close-up images of gypsum on the periphery of the pyrite nodule, illustrating the latest formed authigenic pyrite and greigite (G) grains that grew on the gypsum.

gates, euhedral pyrite crystals are commonly observed as overgrowths on early diagenetic pyrite framboids (Fig. 6d,e). As described above for mechanism 4, the presence of framboidal and euhedral pyrite in the same sample is consistent with evolution of pore waters with framboidal pyrite forming before euhedral pyrite [25].

Clear evidence concerning an additional remagnetization mechanism is available in only a few samples in which pyrite nodules are observed (e.g., Fig. 6f–i). The nodules have dimensions of 0.5–1 mm, with the centres consisting of microcrystalline pyrite (Fig. 6g). It is not clear whether these nodules grew during early or later diagenesis. Early diagenetic growth of large pyrite nodules (30–70 cm across) has been reported [25], so an early origin cannot be precluded in this case. Regardless, the nodules are surrounded and overgrown by amorphous gypsum ($CaSO_4.2H_2O$) (Fig. 6f, h). The variably corroded edges of the pyrite, and the halo around the nodule, which is indicative of a fluid–rock interaction, suggest that the gypsum grew as a result of chemical reactions involving the underlying pyrite. Another generation of iron sulphide grains appears to have grown even later on the outer edges of the gypsum, including relatively coarser-grained pyrite and finer-grained greigite (Fig. 6h,i). Microtextural evidence for the late growth of this greigite after gypsum can explain the observed remagnetization.

Gypsum usually forms in evaporitic environments, however, it has been occasionally observed together with pyrite in anoxic [46] and oxic [47] marine sediments. Siesser and Rogers [46] inferred that the two phases grew during similar pore water conditions when seawater sulphate was available for reduction to sulphide as well as to react with waters supersaturated with carbonate ions. The only observation of gypsum in the paleo-Tiber sediments is in association with pyrite nodules. The microtextural relationships suggest that the sulphate in the gypsum was derived from the sulphide in the pyrite (Fig. 6f). For this sulphate to sulphide reaction to occur, pyrite must undergo oxidation. The studied clays were deposited in brackish environments on a coastal plain [44]. Anoxic conditions suitable for pyrite formation were present during deposition of these clays, but the sediments are likely to have been flushed with oxic pore waters during deposition of the intercalated gravels. Oxidation of pyrite nodules is therefore likely to have occurred during sea level low-stands when the aggradational gravels were deposited. Oxidation would release sulphate from the pyrite sulphide and would lower the pH of the immediately surrounding sediment:

$$4FeS + 9O_2 + 6H_2O \Leftrightarrow 4FeO(OH) + 4SO_4^{2-} + 8H^+. \quad (2)$$

Detrital (or biogenic) carbonate grains, which are abundant in the paleo-Tiber sediments, would then dissolve in the locally more acidic interstitial waters, which would have released calcium and bicarbonate:

$$H^+ + CaCO_3 \Leftrightarrow Ca^{2+} + HCO_3^-. \quad (3)$$

Elevated calcium and sulphate levels would have led to supersaturation and precipitation of gypsum on the oxidizing outer surface of pyrite nodules:

$$Ca^{2+} + SO_4^{2-} + 2H_2O \Leftrightarrow CaSO_4.2H_2O \quad (4)$$

(this mechanism for gypsum formation within deep-sea sediments was suggested by Schnitker et al. [48]). During later phases of clay deposition, pore water conditions are likely to have been anoxic. However, terrestrial sediments do not usually contain abundant sulphate and the diffusion pathway of any available sulphate would be long as a result of deposition of intervening gravels. The gypsum on the surface of the pyrite nodules therefore appears to be the source of sulphate for the late-formed greigite and pyrite (Fig. 6h,i). Alternation between anoxic and oxic depositional environments appears to be responsible for the non-steady state diagenesis that produced the observed remagnetization. Changes in pore water chemistry can also occur as a result of marine incursions (associated with relative sea level change) in coastal settings, including lakes located near sea level. Such situations, where greigite appears to have grown substantially later than the time of deposition, have been documented in several cases [49–51]. Detailed SEM investigations would be needed to investigate the mechanism of later greigite growth associated with marine incursions into these lakes.

Late diagenetic remagnetizations involving greigite formation after gypsum have not been docu-

mented before. This mechanism is most likely to occur as a result of non-steady state diagenesis where the chemical composition of pore waters has undergone substantial variations. A variety of forcing events can give rise to non-steady state diagenesis, including large amplitude sea level variations which can affect continental shelf and coastal terrestrial environments.

6. Discussion and conclusions

Chemical reactions occur in sediments because minerals and other materials such as organic matter are out of equilibrium with their environment [e.g., [20]]. Standard geochemical classification schemes (e.g., Fig. 1) can be used to make inferences about diagenesis based on the presence of authigenic mineral phases that formed during diagenetic decomposition of organic matter. It is worth noting that all of the authigenic minerals that have been observed in this study have been documented in more organic-rich coal deposits [e.g., [52]]. While our detailed petrographic work provides the first systematic documentation of the magnetic implications of this range of mineralogical transformations, the fact that these transformations occur should not be surprising.

In standard diagenetic redox zonation models, one might normally expect greigite to form rapidly during early diagenesis. However, as shown by the number of mechanisms documented above for causing remagnetizations via growth of greigite, it is clear that multiple forcing events are capable of disrupting this steady-state diagenetic progression. The keys to greigite formation are the availability of reactive iron and a source of limited dissolved sulphide [e.g., [2,11]]. If these reactants are available as a result of disruption of pore water conditions away from the expected steady-state progression, then greigite can apparently form at any time during diagenesis. Several forcing mechanisms have been suggested to account for disruption of steady-state pore water conditions in the context of greigite neoformation. These include hydrocarbon seepage [53], gas hydrate migration [54], anaerobic methane oxidation [55,56], tectonic deformation and associated fluid migration [22,57], glacio-tectonic deformation and associated fluid migration [18], convection of sulphate-bearing seawater in the vicinity of cold vent sites/ mud volcanoes [58], migration of sulphate from deep geological reservoirs such as Messinian evaporates in the Mediterranean [16], large amplitude sea level change in continental shelf sediments and associated changes in the subsurface position of the freshwater/seawater interface [18,24], and non-steady-state diagenesis associated with cyclic variation of bottom water oxygenation [59] or with submarine landslide events [60]. Halbach et al. [57] argued that a single large earthquake event can induce pore water transport that can cause transient, but significant (>1000 yr), perturbations of an otherwise steady state system. This observation and the suggestion by Neretin et al. [56] that the S–Fe chemistry of anoxic sediments can be significantly affected by non-steady-state secondary diagenetic overprints are entirely consistent with our observations and suggest that widespread remagnetizations involving greigite should be common in anoxic sediments. We have found different mechanisms for greigite neoformation each time we have investigated a suspected remagnetization involving greigite. We therefore expect the above-documented catalogue of 5 remagnetization mechanisms and the range of different types of forcing events responsible for remagnetizations to expand with further studies. Recent evidence also suggests that greigite can continue to grow for several thousand years after deposition, even in an apparently undisrupted active depositional setting [19]. Together, these observations suggest that greigite is a problematical mineral for paleomagnetism and environmental magnetism and that its presence should be a cause for concern in studies that require interpretation of syn-depositional geophysical, geochemical, or geological signals.

SEM analysis is a powerful tool for observing the context of authigenic growth of iron sulphide minerals and can provide important evidence concerning the relative timing of greigite formation and can reveal the mechanism by which a sediment was remagnetized. The possibility that multiple mechanisms could give rise to an observed remagnetization demonstrates how useful SEM analysis can be for resolving ambiguities. In contrast, magnetic and bulk geochemical analyses alone or in conjunction do not provide enough information to make a reliable judgement on the remagnetization mechanism. SEM analysis should

therefore become a routine tool in studies where greigite or other magnetic iron sulphide minerals are suspected to be responsible for the paleomagnetic signal.

Acknowledgments

We gratefully acknowledge several colleagues for useful discussions, including Wei-Teh Jiang, Chorng-Shern Horng, Fabio Florindo, Fabrizio Marra, Leonardo Sagnotti, and John Thomson. We thank Richard Pearce for assistance with the SEM and Leonardo Sagnotti and Mark Dekkers for helpful review comments on an earlier version of the ms. This work was partially supported by the Leverhulme Trust.

References

[1] B.J. Skinner, R.C. Erd, F.S. Grimaldi, Greigite, the thio-spinel of iron; a new mineral, Am. Mineral. 49 (1964) 543–555.
[2] R.A. Berner, Sedimentary pyrite formation: an update, Geochim. Cosmochim. Acta 48 (1984) 605–615.
[3] M.A.A. Schoonen, H.L. Barnes, Reactions forming pyrite and marcasite from solution. II: via FeS precursors below 100 °C, Geochim. Cosmochim. Acta 55 (1991) 1505–1514.
[4] Q.W. Wang, J.W. Morse, Pyrite formation under conditions approximating those in anoxic sediments. 1: pathway and morphology, Mar. Chem. 52 (1996) 99–121.
[5] R.T. Wilkin, H.L. Barnes, Formation processes of framboidal pyrite, Geochim. Cosmochim. Acta 61 (1997) 323–339.
[6] L.G. Benning, R.T. Wilkin, H.L. Barnes, Reaction pathways in the Fe–S system below 100 °C, Chem. Geol. 167 (2000) 25–51.
[7] D.E. Canfield, R.A. Berner, Dissolution and pyritization of magnetite in anoxic marine sediments, Geochim. Cosmochim. Acta 51 (1987) 645–659.
[8] D.E. Canfield, R. Raiswell, S.H. Bottrell, The reactivity of sedimentary iron minerals toward sulfide, Am. J. Sci. 292 (1992) 659–683.
[9] C.S. Horng, J.C. Chen, T.Q. Lee, Variation in magnetic minerals from two Plio-Pleistocene marine-deposited sections, southwestern Taiwan, J. Geol. Soc. China 35 (1992) 323–335.
[10] C.S. Horng, M. Torii, K.-S. Shea, S.-J. Kao, Inconsistent magnetic polarities between greigite- and pyrrhotite/magnetite-bearing marine sediments from the Tsailiao-chi section, southwestern Taiwan, Earth Planet. Sci. Lett. 164 (1998) 467–481.
[11] S.J. Kao, C.S. Horng, A.P. Roberts, K.K. Liu, Carbon–sulfur–iron relationships in sedimentary rocks from southwestern Taiwan: influence of geochemical environment on greigite and pyrrhotite formation, Chem. Geol. 203 (2004) 153–168.
[12] E. Tric, C. Laj, C. Jéhanno, J.-P. Valet, C. Kissel, A. Mazaud, S. Iaccarino, High-resolution record of the upper Olduvai transition from Po Valley (Italy) sediments: support for dipolar transition geometry? Phys. Earth Planet. Inter. 65 (1991) 319–336.
[13] A.P. Roberts, G.M. Turner, Diagenetic formation of ferrimagnetic iron sulphide minerals in rapidly deposited marine sediments, South Island, New Zealand, Earth Planet. Sci. Lett. 115 (1993) 257–273.
[14] F. Florindo, L. Sagnotti, Palaeomagnetism and rock magnetism in the upper Pliocene Valle Ricca (Rome, Italy) section, Geophys. J. Int. 123 (1995) 340–354.
[15] R. Thompson, T.J.D. Cameron, Palaeomagnetic study of Cenozoic sediments in North Sea boreholes: an example of a magnetostratigraphic conundrum in a hydrocarbon-producing area, in: P. Turner, A. Turner (Eds.), Palaeomagnetic Applications in Hydrocarbon Exploration, Spec. Publ. - Geol. Soc. Lond., vol. 98, 1995, pp. 223–236.
[16] C. Richter, A.P. Roberts, J.S. Stoner, L.D. Benning, C.T. Chi, Magnetostratigraphy of Pliocene–Pleistocene sediments from the eastern Mediterranean Sea, Proc. ODP, Sci. Res. 160 (1998) 61–74.
[17] W.T. Jiang, C.S. Horng, A.P. Roberts, D.R. Peacor, Contradictory magnetic polarities in sediments and variable timing of neoformation of authigenic greigite, Earth Planet. Sci. Lett. 193 (2001) 1–12.
[18] L. Sagnotti, A.P. Roberts, R. Weaver, K.L. Verosub, F. Florindo, C.R. Pike, T. Clayton, G.S. Wilson, Apparent magnetic polarity reversals due to remagnetization resulting from late diagenetic growth of greigite from siderite, Geophys. J. Int. 100 (2005) 89–100.
[19] J. Liu, R.X. Zhu, A.P. Roberts, S.Q. Li, J.-H. Chang, High-resolution analysis of early diagenetic effects on magnetic minerals in post-Middle-Holocene continental shelf sediments from the Korea Strait, J. Geophys. Res. 109 (2004) B03103, doi:10.1029/2003JB002813.
[20] R.A. Berner, A new geochemical classification of sedimentary environments, J. Sediment. Petrol. 51 (1981) 359–365.
[21] P.N. Froelich, G.P. Klinkhammer, M.L. Bender, N.A. Luedtke, G.R. Heath, D. Cullen, P. Dauphin, D. Hammond, B. Hartman, V. Maynard, Early oxidation of organic matter in pelagic sediments of the eastern equatorial Atlantic: suboxic diagenesis, Geochim. Cosmochim. Acta 43 (1979) 1075–1090.
[22] R. Weaver, A.P. Roberts, A.J. Barker, A late diagenetic (synfolding) magnetization carried by pyrrhotite: implications for paleomagnetic studies from magnetic iron sulphide-bearing sediments, Earth Planet. Sci. Lett. 200 (2002) 371–386.
[23] D. Rickard, M.A.A. Schoonen, G.W. Luther III, The chemistry of iron sulfides in sedimentary environments, in: V. Vairavamurthy, M.A.A. Schoonen (Eds.), Geochemical Transformations of Sedimentary Sulfur, American Chemical Society Symposium Series, vol. 612, 1995, pp. 168–193.
[24] H. Oda, M. Torii, Sea-level change and remagnetization of continental shelf sediments off New Jersey (ODP Leg 174A): magnetite and greigite diagenesis, Geophys. J. Int. 156 (2004) 443–458.

[25] R. Raiswell, Pyrite texture, isotopic composition and the availability of iron, Am. J. Sci. 282 (1982) 1244–1263.
[26] R. Raiswell, Q.J. Fisher, Mudrock-hosted carbonate concretions: a review of growth mechanisms and their influence on chemical and isotopic composition, J. Geol. Soc. (Lond.) 157 (2000) 239–251.
[27] A.P. Roberts, G.S. Wilson, F. Florindo, L. Sagnotti, K.L. Verosub, D.M. Harwood, Magnetostratigraphy of lower Miocene strata from the CRP-1 core, McMurdo Sound, Ross Sea, Antarctica, Terra Antart. 5 (1998) 703–713.
[28] D.T. Rickard, Synthesis of smythite-rhombohedral Fe_3S_4, Nature 218 (1968) 356–357.
[29] Y. Furukawa, H.L. Barnes, Reactions forming smythite, Fe_9S_{11}, Geochim. Cosmochim. Acta 60 (1996) 3581–3591.
[30] R.E. Krupp, Smythite, greigite, and mackinawite: new observations on natural low-temperature iron sulfides, in: M. Pagel, J.L. Leroy (Eds.), Source, transport and deposition of metals, Balkema, Rotterdam, 1991, pp. 193–195.
[31] J.C. Baker, C.R. Fielding, Diagenesis of glacimarine Miocene strata in CRP-1, Antarctica, Terra Antart. 5 (1998) 647–653.
[32] R. Raiswell, A geochemical framework for the application of stable sulphur isotopes to fossil pyritization, J. Geol. Soc. (Lond.) 154 (1997) 343–356.
[33] D. Postma, R. Jakobsen, Redox zonation: equilibrium constraints on the Fe(III)/SO_4-reduction interface, Geochim. Cosmochim. Acta 60 (1996) 3169–3175.
[34] K. Pye, J.A.D. Dickson, N. Schiavon, M.L. Coleman, M. Cox, Formation of siderite–Mg–calcite–iron sulphide concretions in intertidal marsh and sandflat sediments, north Norfolk, England, Sedimentology 37 (1990) 325–343.
[35] M. Claps, F.S. Aghib, Carbonate diagenesis in Miocene sediments from CRP-1, Victoria Land Basin, Antarctica, Terra Antart. 5 (1998) 655–660.
[36] D. Postma, The occurrence and chemical composition of recent Fe-rich mixed carbonates in a river bog, J. Sediment. Petrol. 47 (1977) 1089–1098.
[37] K. Pye, Marshrock formed by iron sulphide and siderite cementation in saltmarsh sediments, Nature 294 (1981) 650–652.
[38] M. Krs, F. Novák, M. Krsová, P. Pruner, L. Kouklíková, J. Jansa, Magnetic properties and metastability of greigite-smythite mineralization in brown-coal basins of the Krusné hory Piedmont, Bohemia, Phys. Earth Planet. Inter. 70 (1992) 273–287.
[39] R.E. Krupp, Phase relations and phase transformations between the low-temperature iron sulphides mackinawite, greigite, and smythite, Eur. J. Mineral. 6 (1994) 265–278.
[40] R.C. Erd, H.T. Evans Jr., D.H. Richter, Smythite, a new iron sulfide, and associated pyrrhotite from Indiana, Am. Mineral. 42 (1957) 309–333.
[41] F. Novák, J. Jansa, Authigenic smythite and pyrrhotite in the upper part of the Sokolov Formation (the Sokolov Basin, Czechoslovakia), Bull. Geol. Surv., Prague 67 (1992) 235–244.
[42] V. Hoffmann, Mineralogical, magnetic and Mössbauer data of smythite (Fe_9S_{11}), Stud. Geophys. Geod. 37 (1993) 366–380.
[43] J. Schneider, H. de Wall, A. Kontny, T. Bechstadt, Magnetic susceptibility variations in carbonates of the La Vid Group (Cantabrian Zone, NW-Spain) related to burial diagenesis, Sediment. Geol. 166 (2004) 73–88.
[44] F. Marra, F. Florindo, D.B. Karner, Paleomagnetism and geochronology of early Middle Pleistocene depositional sequences near Rome: comparison with the deep-sea $\delta^{18}O$ record, Earth Planet. Sci. Lett. 159 (1998) 147–164.
[45] F. Florindo, F. Marra, D.B. Karner, A.P. Roberts, R. Weaver, Age constraints for glacial terminations IX, VIII and VII from aggradational sequences of the paleo-Tiber River in Rome (Italy), (in preparation).
[46] W.G. Siesser, J. Rogers, Authigenic pyrite and gypsum in South West African continental slope sediments, Sedimentology 23 (1976) 567–577.
[47] M. Briskin, B.C. Schreiber, Authigenic gypsum in marine sediments, Mar. Geol. 28 (1978) 37–49.
[48] D. Schnitker, L.M. Mayer, S. Norton, Loss of calcareous microfossils from sediments through gypsum formation, Mar. Geol. 36 (1980) M35–M44.
[49] I.F. Snowball, R. Thompson, A stable chemical remanence in Holocene sediments, J. Geophys. Res. 95 (1990) 4471–4479.
[50] P. Sandgren, I.F. Snowball, D. Hammarlund, J. Risberg, Stratigraphic evidence for a high marine shore-line during the late Weichselian deglaciation on the Kullen Peninsula, southern Sweden, J. Quat. Sci. 14 (1999) 223–237.
[51] S.M. Wang, S.Y. Hu, E. Appel, X.H. Ma, V. Hoffmann, Z.M. Sun, X.D. Yang, Y. Ma, H.X. Pan, Incursion of sea water into Gucheng Lake detected by magnetic, biologic and chemical data, Phys. Chem. Earth, A 24 (1999) 805–810.
[52] S.V. Vassilev, M.G. Yossifova, C.G. Vassileva, Mineralogy and geochemistry of Bobov Dol coals, Bulgaria, Int. J. Coal Geol. 26 (1994) 185–213.
[53] R.L. Reynolds, M.L. Tuttle, C.A. Rice, N.S. Fishman, J.A. Karachewski, D.M. Sherman, Magnetization and geochemistry of greigite-bearing Cretaceous strata, North Slope Basin, Alaska, Am. J. Sci. 294 (1994) 485–528.
[54] B.A. Housen, R.J. Musgrave, Rock-magnetic signature of gas hydrates in accretionary prism sediments, Earth Planet. Sci. Lett. 139 (1996) 509–519.
[55] S. Kasten, T. Freudenthal, F.X. Gingele, H.D. Schulz, Simultaneous formation of iron-rich layers at different redox boundaries in sediments of the Amazon deep-sea fan, Geochim. Cosmochim. Acta 62 (1998) 2253–2264.
[56] L.N. Neretin, M.E. Böttcher, B.B. Jørgensen, I.I. Volkov, H. Lüschen, K. Kilgenfeldt, Pyritization processes and greigite formation in the advancing sulphidization front in the upper Pleistocene sediments of the Black Sea, Geochim. Cosmochim. Acta 68 (2004) 2081–2093.
[57] P. Halbach, E. Holzbecher, Th. Reichel, R. Moche, Migration of the sulphate–methane reaction zone in marine sediments of the Sea of Marmara—can this mechanism be tectonically induced? Chem. Geol. 205 (2004) 73–82.
[58] P. Henry, X. Le Pichon, S. Lallement, S. Lance, J.B. Martin, J.-P. Foucher, A. Fiala-Medioni, F. Rostek, N. Guilhaumou, V. Pranal, M. Castrec, Fluid flow in and around a mud volcano field seaward of the Barbados

accretionary wedge: results from Manon cruise, J. Geophys. Res. 101 (1996) 20297–20323.
[59] J.C. Larrasoaña, A.P. Roberts, J.S. Stoner, C. Richter, R. Wehausen, A new proxy for bottom-water ventilation based on diagenetically controlled magnetic properties of eastern Mediterranean sapropel-bearing sediments, Palaeogeogr. Palaeoclimatol. Palaeoecol. 190 (2003) 221–242.
[60] M. Zabel, H.D. Schulz, Importance of submarine landslides for non-steady state conditions in pore water systems–lower Zaire (Congo) deep sea fan, Mar. Geol. 176 (2001) 87–99.
[61] S. Kasten, M. Zabel, V. Heuer, C. Hensen, Processes and signals of nonsteady-state diagenesis in deep-sea sediments and their pore waters, in: G. Wefer, S. Mulitza, V. Ratmeyer (Eds.), The South Atlantic in the Late Quaternary: Reconstruction of Material Budgets and Current Systems, Springer-Verlag, Berlin, 2003, pp. 431–459.